International Journal of Automation and Computing 7(1), February 2010, 78-85
DOI: 10.1007/s11633-010-0078-7

A Novel Fuzzy Direct Torque Control System for Three-level Inverter-fed Induction Machine

Shu-Xi Liu[1] Ming-Yu Wang[1] Yu-Guang Chen[2] Shan Li[2]

[1]State Key Laboratory of Power Transmission Equipment & Systems Security and New Technology, Chongqing University, Chongqing 400044, PRC

[2]School of Electronic Information and Automation, Chongqing University of Technology, Chongqing 400050, PRC

Abstract: Diode clamped multi-level inverter (DCMLI) has a wide application prospect in high-voltage and adjustable speed drive systems due to its low stress on switching devices, low harmonic output, and simple structure. However, the problem of complexity of selecting vectors and capacitor voltage unbalance needs to be solved when the algorithm of direct torque control (DTC) is implemented on DCMLI. In this paper, a fuzzy DTC system of an induction machine fed by a three-level neutral-point-clamped (NPC) inverter is proposed. After introducing fuzzy logic, optimal selecting switching state is realized by applying various strategies which can distinguish the grade of the errors of stator flux linkage, torque, the neutral-point potential, and the position of stator flux linkage. Consequently, the neutral-point potential unbalance, the $\mathrm{d}v/\mathrm{d}t$ of output voltage and the switching loss are restrained effectively, and desirable dynamic and steady-state performances of induction machines can be obtained for the DTC scheme. A design method of the fuzzy controller is introduced in detail, and the relevant simulation and experimental results have verified the feasibility of the proposed control algorithm.

Keywords: Multi-level inverter, direct torque control (DTC), fuzzy controller, space voltage vector, induction machine.

1 Introduction

Three-level inverters presented by Nabae[1] and other scholars, also called neutral-point-clamped (NPC) inverters, have created a new research direction for the development of variable frequency adjustable speed equipment toward high power and voltage[2]. Under the same switching frequency condition, a multi-level inverter NPC can increase the capacity of inverters, and decrease high-order harmonics. In order to eliminate the same harmonics, dual-level inverters with pulse width modulation (PWM) control need a high switching frequency, which will result in great loss. On the contrary, the multilevel inverter needs not a high switching frequency, so its efficiency is much higher[3−5]. For those commonly used inverter topologies, the diode clamped multi-level inverter (DCMLI) shows a wide application prospect in medium- or high-voltage adjustable speed drive systems with high performance.

Direct torque control (DTC), as one of the high-performance AC drives, was extended to the field of multi-level inverters in the late 20th century. Its physical process is very clear. The induction machine is studied in the two-phase stationary coordinate system, which replaces the rotating coordinate transformation, and the effect of torque direct control is emphasized. The close-loop control scheme based on DTC, thanks to its advantages such as simple structure and fast torque response, is highly competitive in constructing high-performance adjustable speed drives[6−9].

However, there are a large number of voltage vectors in multi-level inverters. For example, three-level inverters have the number of 3^3 , namely 27, and five-level inverters have the number of 5^3, namely 125; therefore, the complexity of selecting vectors increases when a DTC is implemented on DCMLI. Firstly, the effects on flux linkage and torque are different for different voltage vectors. Secondly, when the voltage vector switches arbitrarily, the output voltage waveforms will be induced to change jumpily, affecting electric insulation of the machine and increasing the loss of switching devices. Finally, due to the motor load, the output of active power will result in imbalance of DC-side capacitors voltage when the capacitors are charged and discharged. The capacitors voltage imbalance, namely, neutral-point potential fluctuating or excursion, will increase output voltage harmonic content, even do damages to the switching devices, and so on. The all above-mentioned will lead to undesirable performances of the machine operation[10−13]. Therefore, all these factors should be considered, when the algorithm of DTC is implemented in induction machine supplied by DCMLI.

A single vector method was used in [14] to implement DTC algorithm. It is simple but does not consider selection of the space voltage vector dynamically according to the flux linkage and torque change. A synthesized vector method, which considered the capacitor voltage balance and obtained a better control effect, was proposed in the DTC algorithm[15]. However, to some extent, it destroys the simplicity of DTC. A fuzzy control method was adopted in [16], but it did not consider the neutral-point potential balance, leading to not very desirable results.

Therefore, based on three-level NPC voltage source inverter, a novel multilevel DTC with fuzzy logic control realization scheme of induction machine is presented in this paper. After introducing fuzzy logic[17], voltage vectors are selected by applying various strategies which can distinguish the grade of the errors of stator flux-linkage, torque and the neutral-point potential. The basic principle is that the control of torque and flux linkage of the induction machine has the first priority. That is to say that for big errors of torque and flux linkage, it is supposed to select long or

Manuscript received March 13, 2009; revised May 27, 2009

medium vector, and the utilization ratio of the DC voltage increases. Of course, the vector switching should avoid the phase voltage jumping. On the contrary, for very small errors (or close to zero) of torque and flux linkage, it is supposed to select short vector, and the control of neutral-point potential should be taken into account. In order to restrict the fluctuation of capacitor voltage, the redundant short vectors are made full use because of the opposite effect on the capacity voltage. Thus, in this way, it is feasible to restrict the imbalance of neutral-point potential effectively in tolerance, to limit the $\mathrm{d}v/\mathrm{d}t$ of output voltage, to decrease the switching loss, and to obtain desirable speed adjusting characteristics. Finally, the simulation studies are performed according to the proposed strategy. Both simulation and real experimental results indicate that the fuzzy DTC control system based on DCMLI can achieve better static and dynamic performances.

2 The fuzzy direct torque control system

2.1 System structure

Fig. 1 shows the block diagram of a three-level fuzzy DTC system of an induction machine. The three-phase output voltage waveforms are generated by various switching combinations of the switches. The NPC three-level inverter and the induction machine are connected directly, and output transformer or filter is not necessary.

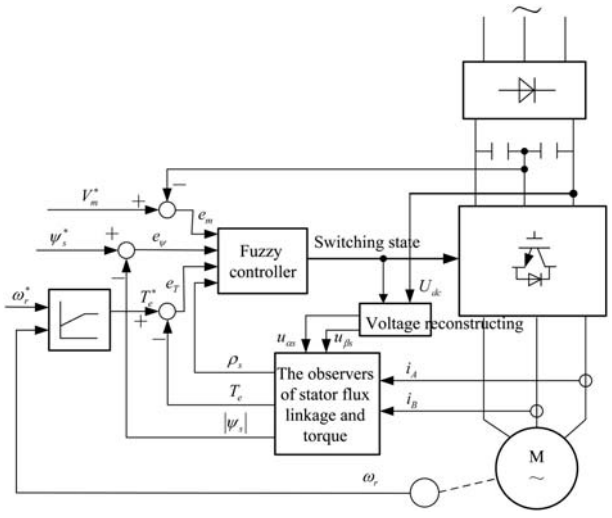

Fig. 1 The schematic block diagram of DTC supplied by three-level inverter

It can be seen that the induction machine stator windings are connected in star-type; only two phase currents are needed to measure, such as i_A and i_B; the third phase current can be calculated by formula $i_C = -i_A - i_B$. The observer of stator flux linkage and torque is employed to implement the coordinate transformation (from three phase to two phase of stator current) and to observe the values of the stator flux linkage and electromagnetic torque, i.e., to obtain the modulus $|\psi_s|$ of flux-linkage vector $\bar{\psi}_s$ and its position angle ρ_s, and electromagnetic torque T_e. The calculation formulae are shown as follows:

$$\psi_{\alpha s} = \int (u_{\alpha s} - i_{\alpha s} R_s)\mathrm{d}t \tag{1}$$

$$\psi_{\beta s} = \int (u_{\beta s} - i_{\beta s} R_s)\mathrm{d}t \tag{2}$$

$$|\psi_s| = \sqrt{\psi_{\alpha s}^2 + \psi_{\beta s}^2} \tag{3}$$

$$\rho_s = \arctan \frac{\psi_{\beta s}}{\psi_{\alpha s}} \tag{4}$$

$$T_e = n_p(i_{\beta s}\psi_{\alpha s} - i_{\alpha s}\psi_{\beta s}) \tag{5}$$

where n_p is the number of pole pairs, R_s is the resistance of stator windings, ρ_s is the position angle of stator flux linkage, $u_{\alpha s}$, $u_{\beta s}$, $i_{\alpha s}$, $i_{\beta s}$, $\psi_{\alpha s}$, and $\psi_{\beta s}$ are the components of stator voltage, stator current, and stator flux linkage in two-phase stator stationary reference frame (α, β), respectively, and $u_{\alpha s}$ and $u_{\beta s}$ may be re-constructed according to the DC source and the switching states of the inverter.

In Fig. 1, e_ψ, e_T, and e_m are the errors of stator flux linkage, electromagnetic torque, and neutral-point potential, respectively, i.e., $e_\psi = \psi_s^* - |\psi_s|$, $e_T = T_e^* - T_e$, and $e_m = V_m^* - V_m$, where ψ_s^* is the reference input of stator flux linkage, T_e^* is the reference input of torque, and V_m^* and V_m are the reference input and measuring value of neutral-point potential, respectively. With e_ψ, e_T, e_m, and the position angle of stator flux linkage ρ_s being the input of fuzzy controller, through fuzzifying, rule inferring, and defuzzifying, the output is the switching states of the three-level NPC inverter which drives the machine to run.

2.2 Three-level voltage vector and DTC

The main circuit of diode clamped three-level NPC inverter is shown in Fig. 2.

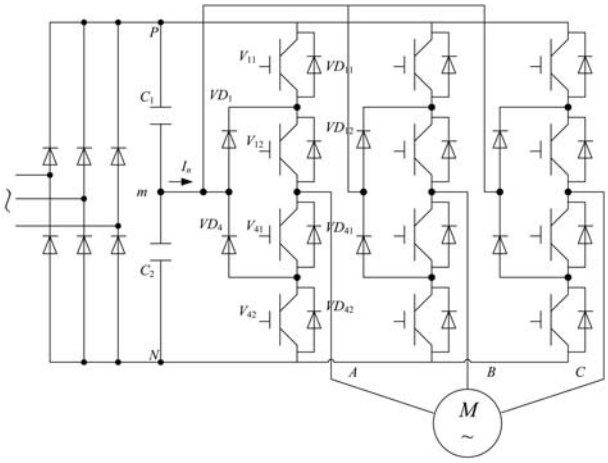

Fig. 2 The main circuit of three-level AC speed-adjusting converter

The AC source is rectified into DC source, and the DC bus capacitor is split into two ones, providing a neutral-point "m". The two capacitors not only act on filtering but also provide voltage supporting. Each arm of the inverter is made up of 4 insulated gate bipolar transistors (IGBTs) devices, and the diodes are connected to the neutral point,

with VD_1 and VD_4 being the clamping diodes. The advantage of the inverter is that the circuit topology is simple, and the output is connected to the machine directly, with no transformer needed. The voltage stress of switching device is only the half of the DC bus voltage, so it is easy to extend the capacity of the inverter. The disadvantages are as follows: 1) more devices are needed; 2) the control algorithm gets more complicated along with the increase in levels; and 3) the neutral-point potential fluctuates easily.

A three-level inverter is characterized by $3^3 = 27$ switching states as indicated in Fig. 3, where the space voltage vector diagram for the three-level inverter is divided into twelve sectors (S_1, S_2, S_3, $\cdots$, S_{12}). There are 24 active states and three zero states lying at the center of the hexagon. According to the modulus of each vector, the 27 vectors are divided into four classes: long vectors V_1–V_6, medium vectors V_7–V_{12}, short vectors V_{13}–V_{18}, and zero vector V_0. The redundancy degree of long and medium vectors is one, and the redundancy degrees of short vectors and zero vector are two and three, respectively.

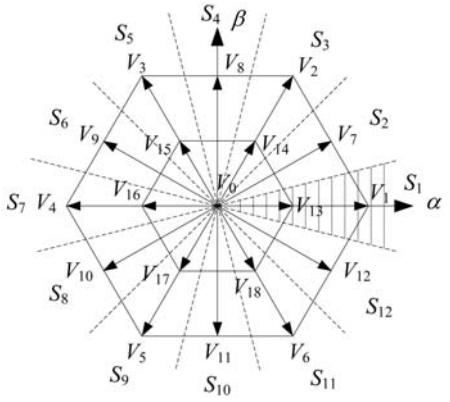

Fig. 3 Space vector graph of a three-level inverter

The conventional three-level DTC, firstly utilizes the diagonal between the adjacent medium vector and long vector to divide the space voltage vector diagram for the three-level inverter into the twelve sectors, i.e., S_1–S_{12}, and then selects the desired voltage vectors according to the errors of torque and the stator flux linkage. Taking the stator flux linkage located in sector S_1 as an example, the selected voltage vectors are summarized in Table 1.

Table 1 Selected voltage vectors when stator flux is located in sector S_1

Object	Selected voltage vector
flux-linkage↑, torque↑	V_2, V_7, V_{14}
flux-linkage↑, torque↓	V_6, V_{12}, V_{18}
flux-linkage↓, torque↑	V_3, V_9, V_{15}
flux-linkage↓, torque↓	V_5, V_{10}, V_{17}

In Table 1, "↑" denotes increasing, and "↓" denotes decreasing. It can be seen from Table 1 that there are three vectors to be selected when a control objective is applied to the torque and the stator flux linkage. Considering the redundancy degree of short vector, i.e., each short vector corresponds to two switching states, therefore, there are four likely switching states to be selected. Through further analysis, it can be seen that the vector affects the torque and flux linkage with the variation of the modulus and direction of the selected vector. For example, to increase the torque and flux linkage, V_2, V_7, and V_{14} can be selected, but the action on the increasing torque of V_2 is the biggest, the action on the increasing flux linkage of V_7 is the biggest, etc.

In general, in order to decrease the torque ripple, the vector adjacent the sector should be considered firstly. At the same time, it is important to avoid switching jump when using the optimal vector table; otherwise, the switching loss and output voltage $\mathrm{d}v/\mathrm{d}t$ will increase, leading to the decrease in system reliability. Therefore, the selected vector maybe a middle value, and sometimes, some transition vectors should be inserted to avoid output voltage jumping, and to decrease $\mathrm{d}v/d\mathrm{t}$. This question should be paid more attention especially when three-level inverters are applied to high-voltage and power occasions. From the above, when a DTC is implemented in DCMLI, all the factors should be considered. It is difficult to select the vectors; however, fuzzy control shows its superiority to some extent.

3 The design of fuzzy controller

3.1 The structure of fuzzy controller

As shown in Fig. 1, e_ψ, e_T, e_m and the position angle of stator flux linkage ρ_s are the inputs of fuzzy controller; the output is the switching states S. Fuzzify e_ψ, e_T, e_m, and ρ_s into fuzzy variables E_ψ, E_T, E_m, and θ when introducing fuzzy logic. The membership functions for the torque error, stator flux-linkage error, neutral-point potential error, and stator flux-linkage position are shown in Fig. 4.

The linguistic terms used for stator flux error and neutral-point potential error are N (negative error), Z (zero error), and P (positive error). For the torque error, the terms used are NL (negative large error), NS (negative small error), Z (zero error), PS (positive small error), and PL (positive large error). The universe of discourse of the position angle of flux linkage has been divided into twelve fuzzy sets (θ_1–θ_{12}). It can be seen that the linguistic terms of torque are more than that of the flux linkage. The torque constant control is the foremost, and then under this premise, some errors of the flux linkage are inessential. After introducing fuzzy logic, by distinguishing the grades of e_ψ, e_T, and e_m, different strategies are applied to selecting long vector, medium vector, short vector, and zero vector. Optimal selecting of switching states improves the system performances.

This fuzzy controller considers the vector selecting when neutral-point potential fluctuates. Busquets-Monge[10] analyzed the three-level inverter switching states affecting the neutral-point potential in detail, and pointed that long and zero vectors have no effect on neutral-point potential. However, the switching states of medium vectors and short vectors imply that at least one phase output is connected to zero bus, and a loop is formed between positive or/and negative bus. Therefore, the capacitors will be induced to charge and discharge, leading to the fluctuations of neutral-point potential.

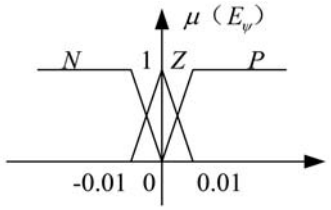

(a) The membership function of E_ψ

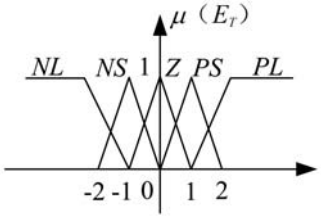

(b) The membership function of E_T

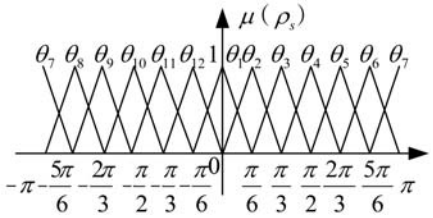

(c) The membership function of ρ_s

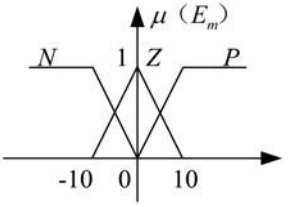

(d) The membership function of E_m

Fig. 4 The distributions of membership functions for all fuzzy variables

At present, the control methods for the balance of neutral-point potential are classified into three types approximately, i.e., passive control, active control, and lag control[3]. The method presented in this paper belongs to lag control. The redundancy degree of short vector is two, corresponding to two switching states, and the influence on DC side capacitors voltage is the opposite of the two switching states. Making use of this characteristic and detecting the direction of the neutral line current, we can make DC voltages of two capacitors almost equal.

The output variable of the fuzzy controller is the inverter state S. In a voltage source inverter, only a defined number of different switching states are possible. Thus, the output variable is discrete. Therefore, the definition of a membership distribution is not necessary for the output variable. The output is a clear variable, made up of 27 separate switching states corresponding to nineteen voltage vectors, and its domain is $\{0, 1, \cdots, 18\}$.

When short and zero vectors are needed, because their redundancies are greater than one, the desired vector should be selected according to the principle of the least switching number, and the detailed method is shown as follows. When $S_k = 0$, where k denotes the k-th sample period, then the output S_{k-1} at last sample time is utilized. If $S_{k-1} = ppo$, then ppp is selected, where p denotes the output connected to positive bus and o denotes the output connected to the neutral point m. If $S_{k-1} = oon$, where n denotes the output connected to negative bus, then ooo is selected. In general, short and zero vectors are utilized to avoid high-voltage changing, to decrease switching loss and to restrict the neutral-point potential in tolerance.

3.2 The rule sets of fuzzy control

The acquirement of fuzzy control rules is based on control experiences of DTC and detailed analysis on the inverter switching states. According to the space voltage vector diagram, suppose that the stator flux linkage rotates anti-clockwise and is located in sector S_2 (namely $15^\circ < \rho_s < 45^\circ$). For example, Fig. 5 can be used to analyze and obtain the needed fuzzy rule sets.

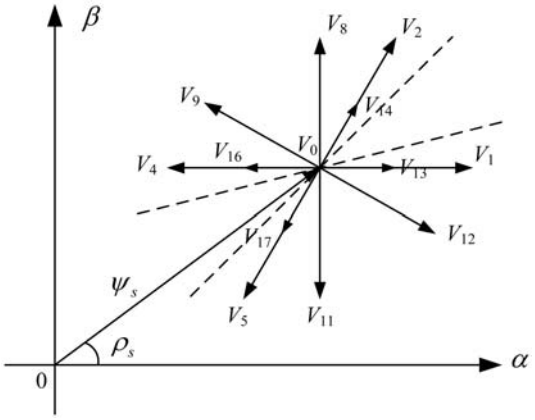

Fig. 5 Selection of the optimum switching voltage vectors

It can be seen that long vectors V_1, V_2, medium vectors V_8, V_{12}, and short vectors V_{13}, V_{14} will increase the flux linkage, while long vectors V_4, V_5, medium vectors V_9, V_{11}, and short vectors V_{16}, V_{17} will decrease the flux linkage. On the other hand, long vectors V_2, V_4, medium vectors V_8, V_9, and short vectors V_{14}, V_{16} will increase the torque, while long vectors V_1, V_5, medium vectors V_{11}, V_{12}, and short vectors V_{13}, V_{17} will decrease the torque.

In summary, selecting V_1 will accelerate the flux-linkage increase and decelerate the torque decrease, selecting V_{12} will decelerate the flux-linkage increase and accelerate the torque decrease, selecting V_{13} will decelerate the flux-linkage increase and the torque decrease, etc. The other vectors are not analyzed one by one. The following basic principles should still be emphasized when designing the fuzzy rules. In order to satisfy the requirement of torque and flux linkage and to decrease harmonics and the ripple of torque, the vectors should be selected near the flux linkage and to avoid the output voltage jump, which can be done by inserting short and zero vectors as the transition vector at a proper time, and so on. When extended to the other sectors, the whole fuzzy control rules can be obtained, including 540 rules at least.

The above fuzzy control rules can be described by e_ψ, e_T, e_m, and S, where the i-th rule can be expressed as follows:

$$\text{if } E_\psi = A_i \text{ and } E_T = B_i \text{ and } \theta = C_i$$
$$\text{and } E_m = D_i \text{ then } S = N_i \tag{6}$$

where A_i, B_i, C_i, D_i, and N_i are fuzzy or explicit variables which belong to the universe of discourse for E_ψ, E_T, E_m, θ, and S, respectively.

3.3 The course of fuzzy reasoning

The inference method used in this paper is Mamdani′s procedure based on max-min algorithm. The outputs are obtained directly, and the maximum criterion method is used for defuzzification. The membership function of output switching state is expressed in the following form.

$$\mu_s(s) = \max_{i=1}^{540}[\mu_{A_i}(E_\psi) \wedge \mu_{B_i}(E_T) \wedge \mu_{C_i}(\theta) \wedge \mu_{D_i}(E_m) \wedge \mu_{S_i}(S)] \tag{7}$$

where μ_{A_i}, μ_{B_i}, μ_{C_i}, and μ_{D_i} are the membership of A_i, B_i, C_i, and D_i, $\mu_{s_i}(s)$ is the membership values of the switching states output, and "∧" is the minimum operator. The value of fuzzy output, which has the maximum possibility distribution, is used as the control output. Then, the nonlinear profile of the fuzzy controller output is obtained, as shown in Fig. 6.

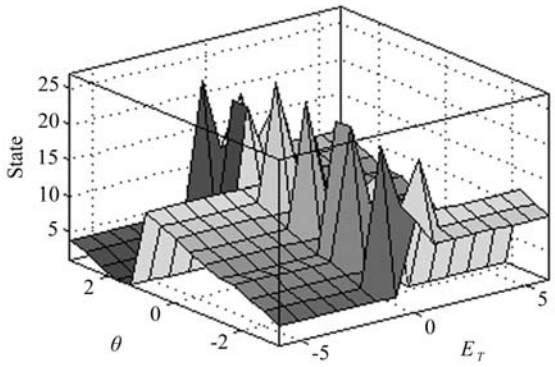

Fig. 6 The nonlinear profile of the fuzzy controller

4 Simulation and experiments

In order to verify the feasibility of the fuzzy DTC algorithm proposed in the paper, simulations and experiments were performed for the induction motor supplied by diode clamped three-level inverter. These experiments included speed tracking at different loads, speed step responses, antidisturbances, etc. Simulation model is shown in Fig. 1, in which the main circuit is made up of rectifier, the filter capacitors at the DC side, inverter and an induction motor, and the control circuit is made up of flux linkage and torque observer, the voltage reconstructing unit, speed proportional-integral (PI) controller and fuzzy controller.

The parameters of the induction motor were as follows: stator resistance $R_s = 3.2\,\Omega$, rotor resistance $R_r = 3.5119\,\Omega$, stator leakage inductance $L_{1s} = 0.027365$ H, rotor leakage inductance $L_{1r} = 0.027365$ H, mutual inductance $L_m = 0.6222$ H, $J = 0.12\,\text{kg}\cdot\text{m}^2$, $p = 3$, and $C_1 = C_2 = 220\,\mu$F. The control period was 100μs, and the fundamental frequency was 50 Hz.

Simulation results for the fuzzy DTC algorithm of induction machine are shown in Fig. 7. Fig. 7 (a) was the wave of stator flux linkage, and the set point was 0.9 Wb. Fig. 7 (b) shows the speed step response at empty load; the system was at static excitation stage to build rated rotor flux before $t = 0.1$ s.

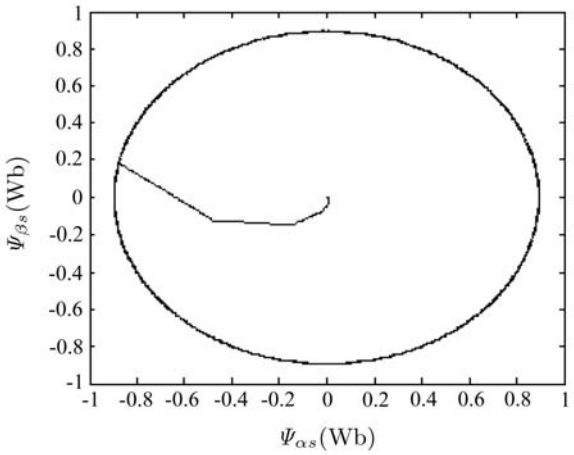

(a) Stator flux-linkage wave

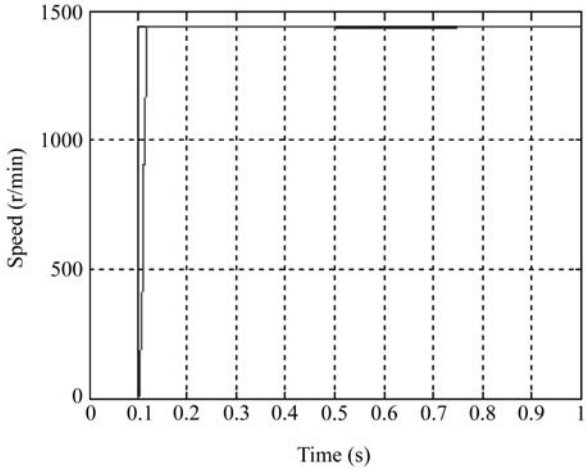

(b) Rotor speed wave

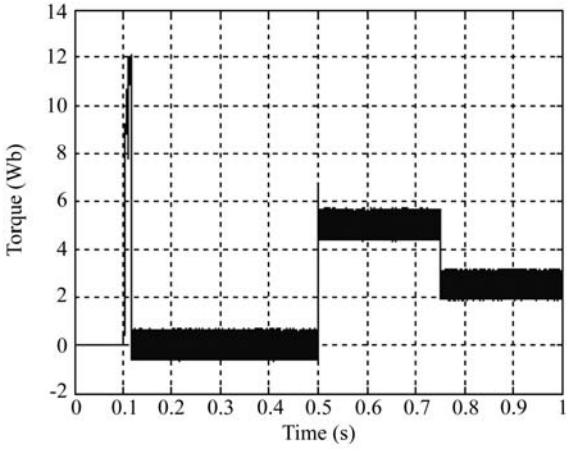

(c) Electromagnetic torque wave

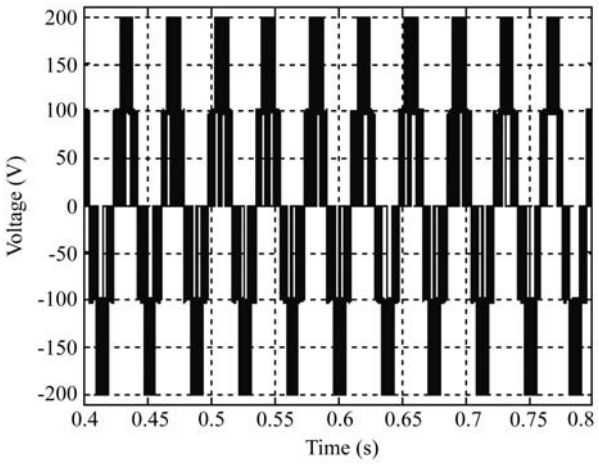

(d) Line voltage wave

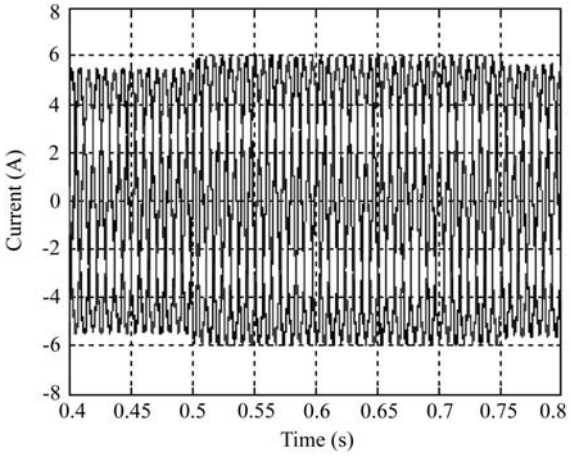

(e) Three-phase stator current wave

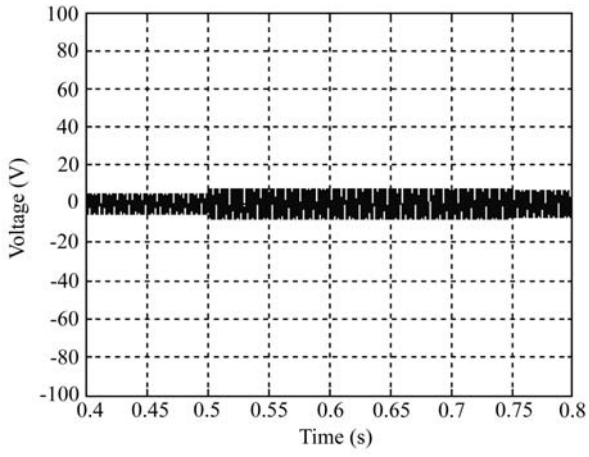

(f) Neutral-point potential wave

Fig. 7 The simulation results of the system

At time $t = 0.1$ s, the reference speed stepped from 0 to 1440 rpm, the speed PI controller of the control system was quickly saturated, and motor rotor speed reached the reference value with the biggest acceleration under the action of biggest torque, as shown in Fig. 7 (c). About at the time $t = 0.12$ s, rotor speed was near the given value, and the speed controller quickly exited saturation, reaching a steady operation quickly. At the time $t = 0.5$ s, the load was added suddenly, from 0 N·m to 5 N·m. At the time $t = 0.75$ s, the load torque was suddenly decreased, from 5 N·m to 2.5 N·m, and the torque response was shown in Fig. 7 (c). It can be seen that the motor torque responded quickly to the motor load change. The dynamic fall value of the system was only about 0.3%, and the steady fall value was zero. All these data indicate that the fuzzy DTC system has desirable dynamic and steady performances.

Figs. 7 (d) and (e) give the line voltage of stator windings and the three-phase stator current at steady operation, respectively. It can be seen that the output voltage of multilevel inverter is more close to sine wave, with the output voltage jump reduced. High-order harmonic is very few, which is beneficial to the steady operation for the induction machine.

Fig. 7 (f) is the voltage wave of neutral-point of capacitors in the DC side. It can be seen that the fluctuation of neutral point voltage was restricted effectively to the tolerant. The fluctuation varied with the variation of the load. The bigger the load, the greater the fluctuation magnitude, because of active power output. The charging and discharging currents became large, and the lag control was used; then the fluctuation of neutral-point was restricted but not eliminated completely.

Experiments were performed with the hardware intelligent power module (IPM) and the controller digital single processor (DSP) TMS320F2812, the other equipment including a 50 Hz, four-pole 2.2 kW induction machine, power circuit, and so on. The DC bus was 400 V, and the inverter switching frequency was 10 kHz. The experimental results of the proposed control system are shown in Fig. 8. The rotor speed step response in Fig. 8 (a) shows that the dynamic performance of the DTC drive was not deteriorated by the proposed algorithm for a three-level inverter system. The set value of rotor speed was 1 440 rpm. Fig. 8 (b) is the line voltage V_{ab} and phase current i_{as} (s denoting the stator) of the induction machine at steady state, which is close to ideal sine wave. Fig. 8 (c) is the wave of the neutral-point potential of the three-level inverter at steady state, and it fluctuates slightly.

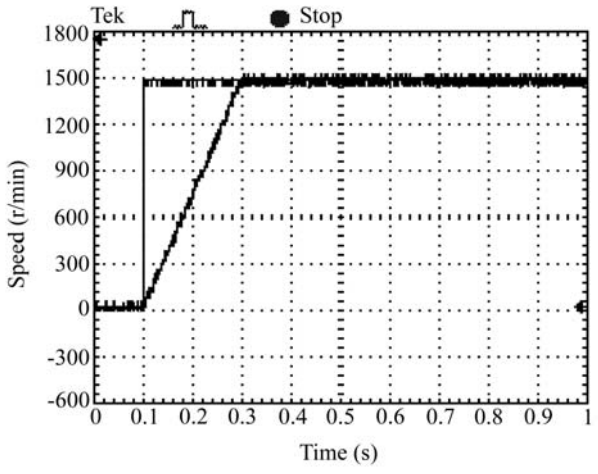

(a) The step response of rotor speed

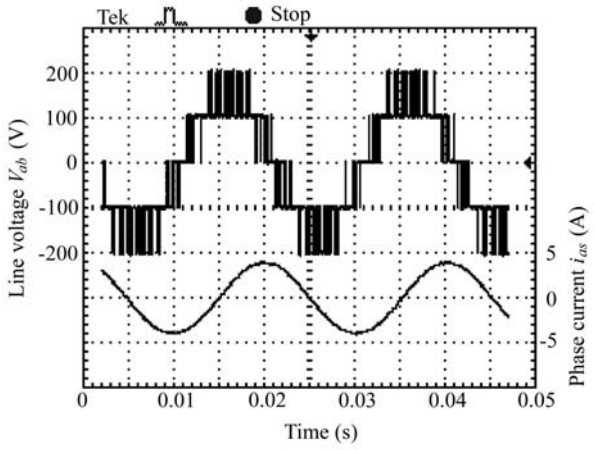

(b) Line voltage V_{ab} and phase current i_{as}

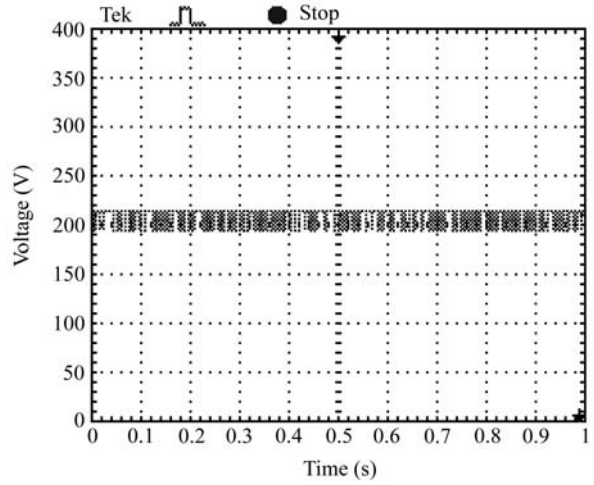

(c) Neutral-point potential wave

Fig. 8 The experimental results of the system

From the above waves, it can be seen that the experimental results were consistent with the simulation results, indicating that the fuzzy DTC algorithm is proper and feasible.

5 Conclusions and future work

DTC is an important alternative method for the induction motor drive system. The main advantage is its high performance and simplicity. When the DTC was implemented in the three-level neutral-point clamped inverter, due to the enhanced possibilities for the inverter state selection in a three-level inverter, a fuzzy logic controller was designed in order to replace the conventional DTC adapted for a three-level inverter based on a table. This approach provides a more accurate selection of the inverter state. Simulations and experimental data of the novel DTC scheme show the reductions of torque ripple and harmonic distortion in both stator currents and voltages. The system has desirable dynamic and steady performances.

The future work will focus on the improvement of the system behavior at low speed, where DTC performance is less satisfactory.

References

[1] A. Nabae, I. Takahashi, H. Akagi. A new neutral-point-clamped PWM inverter. *IEEE Transactions on Industry Applications Society*, vol. 17, no. 5, pp. 518–523, 1981.

[2] B. Wu. *High-power Converters and AC Drives*, Hoboken, New Jersey, USA: IEEE Wiley Press, pp. 33–50, 2006.

[3] J. Rodríguez, J. S. Lai, F. Z. Peng. Multilevel inverters: A survey of topologies, controls, and applications. *IEEE Transactions on Industrial Electronics*, vol. 49, no. 4, pp. 724–738, 2002.

[4] H. Yu. Modeling and control of hybrid machine systems – A five-bar mechanism case. *International Journal of Automation and Computing*, vol. 3, no. 3, pp. 235–243, 2006.

[5] S. Wei, B. Wu, F. Li, C. Liu. A general space vector PWM control algorithm for multilevel inverters. In *Proceedings of the 18th Annual IEEE Applied Power Electronics Conference*, IEEE, Miami, Florida, USA, vol. 1, pp. 562–568, 2003.

[6] J. T. Cao, H. H. Liu, P. Li, D. J. Brown, G. Dimirovski. A study of electric vehicle suspension control system based on an improved half-vehicle model. *International Journal of Automation and Computing*, vol. 4, no. 3, pp. 236–242, 2007.

[7] M. Cirrincione, M. Pucci, G. Scordato, G. Vitale. A low-cost three-level converter for low-power electrical drives with induction motor applied to direct torque control. In *Proceedings of IEEE the 35th Annual Power Electronics Specialists Conference*, IEEE, Aachen, Germany, vol. 6, pp. 4571–4577, 2004.

[8] J. G Williams, G. Liu, S. Chai, D. Rees. Intelligent control for improvements in PEM fuel cell flow performance. *International Journal of Automation and Computing*, vol. 5, no. 2, pp. 145–151, 2008.

[9] S. Busquets-Monge, J. D. Ortega, J. Bordonau, J. A. Beristain, J. Rocabert. Closed-loop control design for three-level three-phase neutral-point-clamped inverter using the optimized nearest three virtual-space-vector modulation. In *Proceedings of the 37th IEEE Power Electronics Specialists Conference*, IEEE, Jeju, Korea, pp. 1–7, 2006.

[10] S. Busquets-Monge, J. Bordonau, D. Boroyevich, S. Somavilla. The nearest three virtual space vector PWM — A modulation for the comprehensive neutral-point balancing in the three-level NPC inverter. *IEEE Power Electronics Letters*, vol. 2, no. 1, pp. 11–15, 2004.

[11] N. Celanovic, D. Boroyevich. A fast space-vector modulation algorithm for multilevel three-phase converters. *IEEE Transactions on Industry Applications*, vol. 37, no. 2, pp. 637–641, 2001.

[12] M. S. S. Ahmed, P. Zhang, Y. J. Wu. Position control of synchronous motor drive by modified adaptive two-phase sliding mode controller. *International Journal of Automation and Computing*, vol. 5, no. 4, pp. 406–412, 2008.

[13] J. H. Suh, C. H. Choi, D. S. Hyun. A new simplified space-vector PWM method for three-level inverters. *IEEE Transactions on Power Electronics*, vol. 16, no. 4, pp. 545–550, 2001.

[14] Y. Li, X. Hou, Z. Tan. Direct torque control of inductor motor fed by three level inverter (I): Single vector method. *Transactions of China Electrotechnical Society*, vol. 19, no. 4, pp. 34–39, 2004. (in Chinese)

[15] L. Lin, Y. Zou, Z. Wang, H. Jin, X. Zou, H. Zhong, X. Zou, H. Zhong. A DTC algorithm of induction motors fed by three-level inverter with neutral-point balancing control. *Proceedings of the CSEE*, vol. 27, no. 3, pp. 46–50, 2007. (in Chinese)

[16] X. del Toro, S. Calls, M. G. Jayne, P. A. Witting, A. Arias, J. L. Romeral. Direct torque control of an induction motor using a three-level direct torque control of an induction motor using a three-level. In *Proceedings of IEEE International Symposium on Industrial Electronics*, IEEE, vol. 2, pp. 923–927, 2004.

[17] S. Liu, T. Li, M. Wang. Two-dimensional fuzzy controller based on memory address mapping. *Chinese Journal of Scientific Instrument*, vol. 29, no. 7, pp. 1436–1440, 2008. (in Chinese)

Shu-Xi Liu received the M. Sc. degree in electrical engineering from Chongqing University, PRC in 2005. He is currently a Ph. D. candidate in Chongqing University, PRC. He is also an associate professor in the Department of Electrical Engineering and Automation at Chongqing University of Technology, PRC.

His research interest includes intelligent drive control technology.

E-mail: shuxi@cqit.edu.cn (Corresponding author)

Ming-Yu Wang received the B. Eng. degree in electrical engineering from Chongqing University, PRC in 1982 and the Ph. D. degree from the Liverpool John Moores University, UK in 1999. He became a member of the Academic Staff, Department of Automation Engineering, Chongqing University in 1982 and was a lecturer there from 1988 to 1993. He was a visiting scholar in the Department of Electrical Engineering, University of Manchester, UK from 1993-1995. He is currently a professor with Chongqing University.

His research interests include power converters, power filters, adjustable speed drives, and vector control of induction machines.

E-mail: eeemwang@tom.com

Yu-Guang Chen received the B. Eng. degree in electrical engineering from Chongqing University, PRC and the M. Eng. degree in mechanical engineering from Xi′an Jiaotong University, PRC. He was a visiting scholar in the School of Science and Technology, Teesside Polytechnic, UK during 1990–1992. He is currently a professor in Chongqing University of Technology, PRC.

His research interests include intelligent control theory and application.

E-mail: cyg6610@cqut.edu.cn

Shan Li received the B. Sc. degree in electrical engineering from Hunan University, PRC in 1985 and the M. Sc. degree in Shaanxi Mechanics College, PRC in 1992. He is currently a professor in Chongqing University of Technology, PRC.

His research interests include power electronics and motion control.

E-mail: lishan@cqut.edu.cn